

Transport of particles by a thermally induced gradient of the order parameter in nematic liquid crystals

M. Škarabot,¹ Ž. Lokar,¹ and I. Muševič^{1,2}

¹*J. Stefan Institute, Jamova 39, SI-1000 Ljubljana, Slovenia*

²*Faculty of Mathematics and Physics, University of Ljubljana, Jadranska 19, SI-1000 Ljubljana, Slovenia*

(Received 20 March 2013; published 3 June 2013)

We demonstrate manipulation and transport of microparticles and even fluorescent molecules by the thermally induced gradient of the order parameter in the nematic liquid crystal. We use IR light absorption of the tightly focused beam of laser tweezers to heat locally a thin layer of the nematic liquid crystal by several degrees. This creates a spatial gradient of temperature of the nematic liquid crystal over separations of several tens of micrometers. We show that a dipolar colloidal particle is attracted into the hot spot of the laser tweezers. The depth of the trapping potential scales linearly with particle radius, indicating that the trapping mechanism is due to elastic self-energy of the distorted nematic liquid crystal around the particle and softening of the elasticity with increased temperature of the liquid crystal. We also demonstrate that this thermal trapping mechanism is efficient down to the nanoscale, as fluorescent molecules are also transported into hotter regions of the liquid crystal. This effect is absent in the isotropic phase, which calls into question particle transport due to the Soret effect.

DOI: [10.1103/PhysRevE.87.062501](https://doi.org/10.1103/PhysRevE.87.062501)

PACS number(s): 61.30.Hn, 61.30.Pq, 68.08.Bc

I. INTRODUCTION

In the past decade, dispersions of microparticles and nanoparticles in liquid crystals (LCs) have been extensively studied both experimentally and theoretically because of the variety of fundamental phenomena observed in these systems and promising applications in optics and photonics. One of the most fascinating phenomena in nematic colloids is the emergence of forces between colloidal particles, which has its origin in the elastic deformation of the LC around colloidal inclusions. These forces are highly anisotropic, they are of long range, and their strength exceeds the forces in water-based colloids for several orders of magnitude. These unusual properties make nematic colloids promising candidates for self-assembly of robust colloidal structures and superstructures with unusual optic and photonic properties.

To study and measure interparticle forces in nematic colloids, one has to trap and manipulate positions of individual micrometer-size particles inside a birefringent liquid medium such as a LC. Efficient and precise methods of trapping and controlled manipulation of microparticles in LCs are therefore essential for the studies of nematic colloids. To this aim, different methods for manipulation of microparticles in LCs have been invented and developed, most of them based on laser tweezers. A tightly focused laser beam was used for manipulating liquid crystal textures [1], switching and spinning LC droplets with circularly polarized tweezers [2–5], and manipulating line defects and measuring their line tension [6]. Laser tweezers were used in low-index nematic LCs to trap and measure colloidal forces between particles with higher refractive index [7,8]. It was demonstrated (surprisingly) that particles with lower refractive index compared to that of the LC could be trapped and manipulated on a microscale [9,10], which made it possible to manipulate any object with arbitrary refractive index using the forbidden trapping mechanism [11–14]. On a macroscopic scale, an external electric field [15–18], nematic-isotropic interfaces [19], or microfluidics [20] were used to transport colloidal particles in the nematic LC.

It was demonstrated some time ago that thermal effects, induced by local optical heating with laser tweezers, generate significant forces on micrometer-size colloidal particles in the nematic liquid crystal (NLC) [21]. Using high-power laser tweezers, an island of the isotropic LC was created, which was separated from the rest of the LC with an interface. Colloidal particles that were positioned close to this isotropic island were attracted to the nematic-isotropic interface. It was also found that these silica colloidal particles with functional surfaces were relatively highly charged in the NLC, which in itself was a surprise. The Soret effect due to directed diffusion in a thermal gradient was ruled out because the effect was not observable in the isotropic phase. It was therefore proposed that the observed force on a colloidal particle was in fact the electric force on charged colloids in the electric field generated by the flexoelectric effect due to the thermal and spatial gradient of the order parameter S around the isotropic island induced. This is one of the possible explanations [22,23].

Related to this colloidal transport in the gradient of the order parameter S is the molecular manipulator reported recently [24]. In that work, spatial variations of the order parameter S were induced by local UV illumination of an azobenzene-doped nematic LC. Due to UV light-induced cis-trans isomerization of dye molecules, the illuminated region developed a gradient of the order parameter S . This region of inhomogeneous orientational order acted as a trap for fluorescent molecules, which were also dissolved throughout the nematic LC. A local increase of the density of fluorescent molecules in the region of decreased order parameter was easily visualized optically. This mechanism is therefore an analog of the thermal Soret effect, where the gradient of the temperature is replaced by the gradient of the molecular concentration that locally alters the magnitude of the order parameter.

In this work we use a focused beam of laser tweezers to heat locally the nematic LC via the absorption of light. Because of the local increase of the temperature, the order parameter of the NLC is locally decreased, which creates a

gradient of the order parameter field. We demonstrate that micrometer-size particles are attracted into the region of the reduced order parameter, which is the same result as already obtained by Tatarkova *et al.* [21]. However, we demonstrate that this structural force is substantial also on the molecular level. When fluorescent molecules are dissolved in the nematic LC instead of micrometer-size colloidal particles, we observe the same effect and the fluorescent molecules are attracted into the region where the temperature is increased and the order parameter is decreased. The effect is not observable in the isotropic phase of the LC, which puts into question the possibility of molecular transport due to the Soret effect. This is therefore a thermal analog of the molecular manipulator demonstrated recently [24] that uses cis-trans isomerization of dye molecules to change the degree of local nematic order.

II. EXPERIMENT

We used two different types of nematic dispersions in our experiments. In the first study, silica microspheres with diameter $2.32\ \mu\text{m}$ (Bangs Laboratories) were dispersed in the nematic liquid crystal 4-pentyl-4'-cyanobiphenyl (5CB) (Nematel) or E12 (Merck) at very low concentrations, typically below 0.01%. The nematic-isotropic phase transition temperature is $T_c = 34^\circ\text{C}$ for 5CB and $T_c = 60^\circ\text{C}$ for E12. Prior to dispersing, the surfaces of silica microspheres were covered with *N,N*-dimethyl-*N*-octadecyl-3-aminopropyltrimethoxysilylchloride (DMOAP) silane (ABCR GmbH), which ensures a very strong perpendicular orientation of LC molecules at the surface. For the second study, molecules of the fluorescent dye rhodamine B octadecyl ester perchlorate (Fluka) were dispersed in 5CB at the concentration of 0.5%.

Glass cells were filled with liquid crystal dispersions using capillary forces. The cells were assembled of two parallel optically transparent indium tin oxide (ITO) -coated glasses covered with a thin layer of a polyimide (PI-2555, Nissan Chemicals). The thickness of the glass was 0.7 mm and the thickness of the ITO layer was $\sim 15\ \text{nm}$. The gap between the glass plates was controlled with mylar spacers and was set to $5\text{--}7\ \mu\text{m}$. The polyimide layer was rubbed unidirectionally to obtain excellent planar alignment of the nematic LC, with directions of the alignment on both surfaces set parallel during the assembly of the cell. The ITO coating was used as an absorber of the laser light at the surface of glasses and provided very good control of the local heating of the LC. We used a laser tweezers setup built around an inverted microscope (Nikon Eclipse, TE2000-U) with an infrared fiber laser operating at $1064\ \text{nm}$ as a light source and a pair of acousto-optic deflectors driven by computerized system (Aresis, Tweez 70) for trap manipulation. The trajectories of the microparticles were video recorded using the Pixelink PLA 741 camera at a frame rate of 40 frames per second. In an off-line analysis, the positions of microparticles were determined by a video-tracking procedure with a typical resolution of particle's position of $\pm 5\ \text{nm}$. To observe the spatial distribution of the fluorescent dye molecules, a highly sensitive camera Rolera MG1 (QImaging) was used with a xenon lamp illumination (Lambda LS, Sutter Instruments). To determine the birefringence of the irradiated LC sample, the spectrum of the transmitted light was measured

between crossed polarizers using an imaging spectrometer (Shamrock SR-500i, Andor).

III. RESULTS AND DISCUSSION

We have observed in a number of experiments that the laser trapping of micrometer-size particles in thin planar LC cells with ITO coating is very efficient over extraordinarily large distances greater than $40\ \mu\text{m}$ at a relatively low power of the laser trap $\approx 30\ \text{mW}$. At this power level no distortions of the LC due to an optically induced Fréedericksz transition was observed. This kind of trapping was observed only in cells made of glasses with an ITO layer, so we conclude that the absorption of laser light in the ITO layer and consequent local heating of the LC are essential for this kind of trapping. To prove this, we analyzed the effect of the laser trap on the birefringence of the thin planar layer of E12 LC under a polarizing microscope. We observed that the thermal equilibrium of the sample was achieved $\approx 2\ \text{s}$ after the laser trap was switched on and therefore all experiments were performed more than $10\ \text{s}$ after switching on the laser tweezers.

Figure 1(a) shows a planar $\sim 5\text{-}\mu\text{m}$ -thick layer of E12 between crossed polarizers aligned at 45° with respect to the

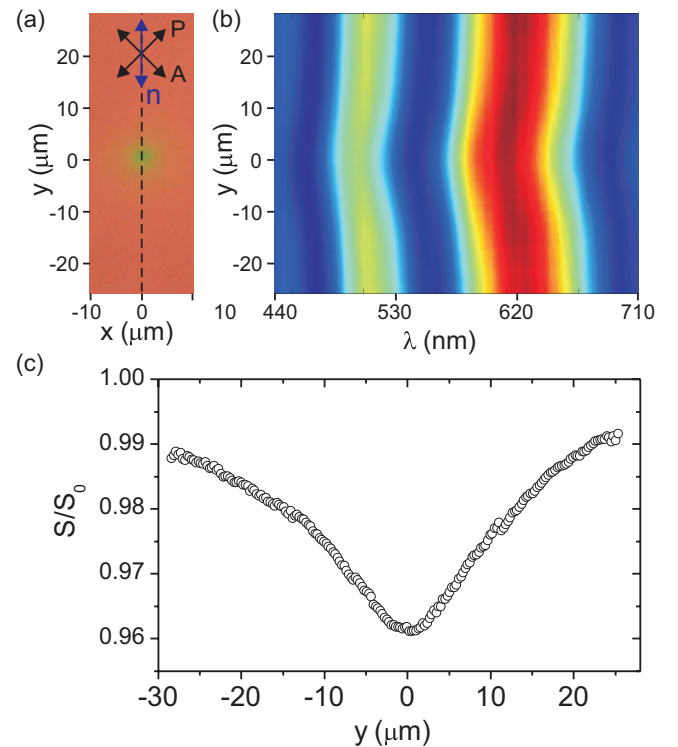


FIG. 1. (Color online) (a) Micrograph of a $\sim 5\text{-}\mu\text{m}$ -thick layer of E12 LC under crossed polarizers locally heated by the laser tweezers with the power of $30\ \text{mW}$. The rubbing direction is at 45° with respect to the polarizers. (b) Wavelength dependence of the intensity of the transmitted light, measured along the dashed line shown in (a) and crossing the center of the trap $x = 0$. The maximum shift of the spectrum is exactly at the center of the trap. (c) Decrease of the order parameter due to the local heating with the focused IR beam, calculated from the measured change of the birefringence along the dashed line in (a).

director, illuminated with a focused 1064-nm beam of the laser trap. One can clearly see that the color of the sample at the position of the laser trap is green shifted with respect to the unperturbed LC, which means that the birefringence is smaller in the region around the laser trap. This local depression of the birefringence is due to the decrease of the order parameter S , which decreases with increasing temperature due to the local laser heating. The decrease of the birefringence was analyzed by measuring the spectrum of the intensity of the transmitted light. Figure 1(b) presents this spectrum measured along the dashed line in Fig. 1(a), crossing the center of the optical trap. Minima and maxima in the spectrum are due to the interference of light passing through the thin birefringent nematic layer. The LC birefringence Δn can be determined by measuring their positions. These extremes are clearly shifted to shorter wavelengths close to the position of the optical trap, where the measured Δn is obviously decreased. It is well known and documented [25] that Δn is proportional to the nematic order parameter S , which means that the order parameter S is lowered at the position of the trap due to the local heating of the LC, caused by absorption of the IR light in the ITO layer. There was no effect of the laser trap on the Δn and S in other experiments, where glasses without an ITO layer were used.

The relative decrease of the order parameter S/S_0 was determined by measuring the decrease of Δn [25]. Its positional dependence along the dashed line in Fig. 1(a) and crossing the optical trap is presented in Fig. 1(c). It is clear that S is minimal at the center of the trap and it is symmetrical around it. The area of the heated LC is relatively large and the decrease of S can be detected at separations as large as $100 \mu\text{m}$ from the trap.

The thermally induced gradient of the order parameter can be used for trapping different kinds of particles dispersed in the nematic LC. In the first experiment we used $2.32\text{-}\mu\text{m}$ microspheres with perpendicular surface anchoring of the LC, dispersed in E12. The colloidal particle is accompanied by a hedgehog point defect and represents an elastic, or topological, dipole [Fig. 2(a)]. When the same laser power is used as in the experiment presented in Fig. 1 (30 mW), a small decrease of the intensity of the transmitted light can be seen at the trap position due to the decrease of the nematic order [Fig. 2(a)], but no reorientation of the director field [Fig. 2(b)]. Typical trapping trajectories are presented in Fig. 2(c), where the trapping trajectories are clearly radial and the trapping is very efficient over large distance from the trap, greater than $40 \mu\text{m}$. This is characteristic of the trapping via a thermally induced spatial gradient of the nematic order.

The trapping force is balanced with the viscous force $F = 6\pi d_{\text{eff}}\eta v$, where d_{eff} is an effective diameter of the colloid, v is its velocity, and η is the liquid crystal viscosity [26]. The product of the effective diameter and viscosity $d_{\text{eff}}\eta$ was determined in a separate experiment by observing the thermal motion of a single colloid [27]. The trapping force is several tenths of a pN at relatively large separation $y \leq 30 \mu\text{m}$ from the trap. The separation dependence of the trapping force is presented in Fig. 2(d) for one experiment, together with the gradient of the order parameter $\Delta S/\Delta y$, which was obtained from measured dependence of S , presented in Fig. 1(c). It is clear that the trapping force is proportional to the gradient of the order parameter, as expected. Figure 2(e) shows rather good

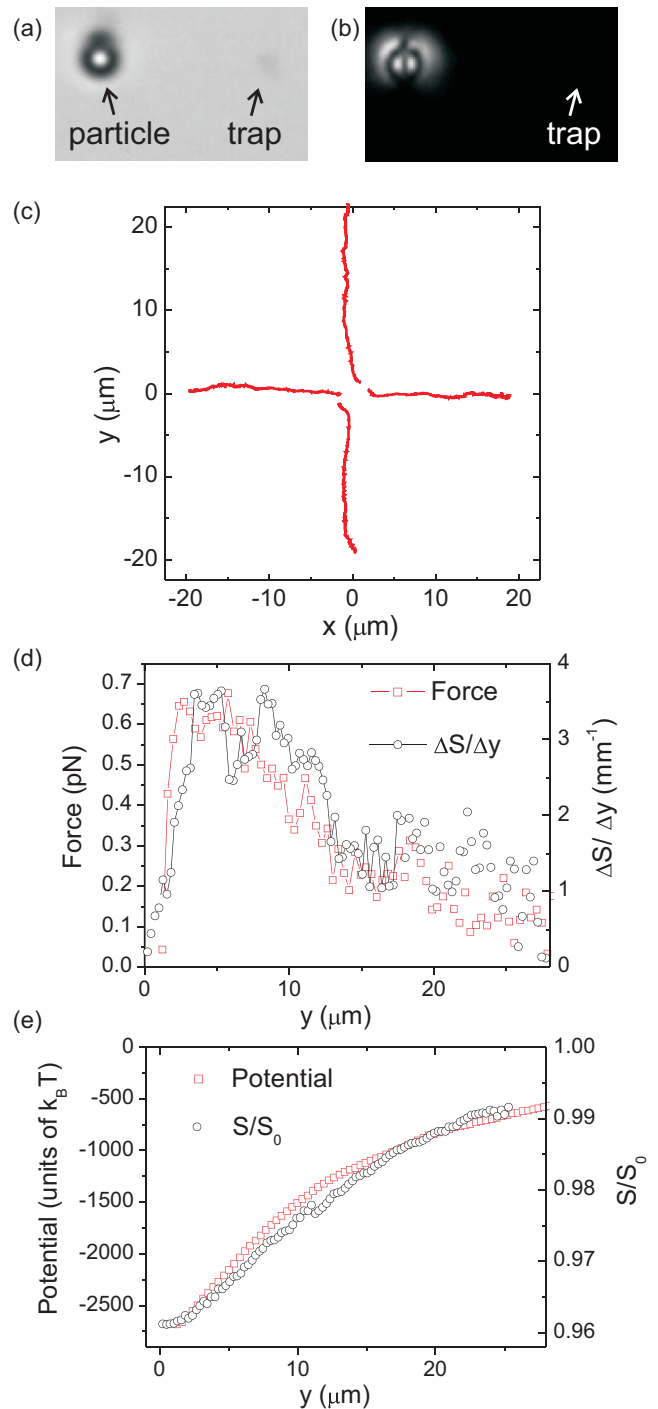


FIG. 2. (Color online) Trapping of $2.32\text{-}\mu\text{m}$ DMOAP-treated microspheres with laser tweezers with the power of 30 mW in a $\sim 5\text{-}\mu\text{m}$ -thick planar layer of E12 nematic LC confined between two ITO-coated glass plates. (a) At the position of the trap a small decrease of the transmitted light can be seen, most likely due to the lensing effect. (b) No reorientation of the nematic order can be observed at the trap position. (c) Trapping trajectories are purely radial. (d) The trapping force was calculated by measuring the velocity of the particle and it is clearly proportional to the gradient of the order parameter, which was calculated from the measured spatial dependence of the birefringence. (e) Trapping potential, calculated as the work of the trapping force (d) along the trajectory and the order parameter profile from Fig. 1(c).

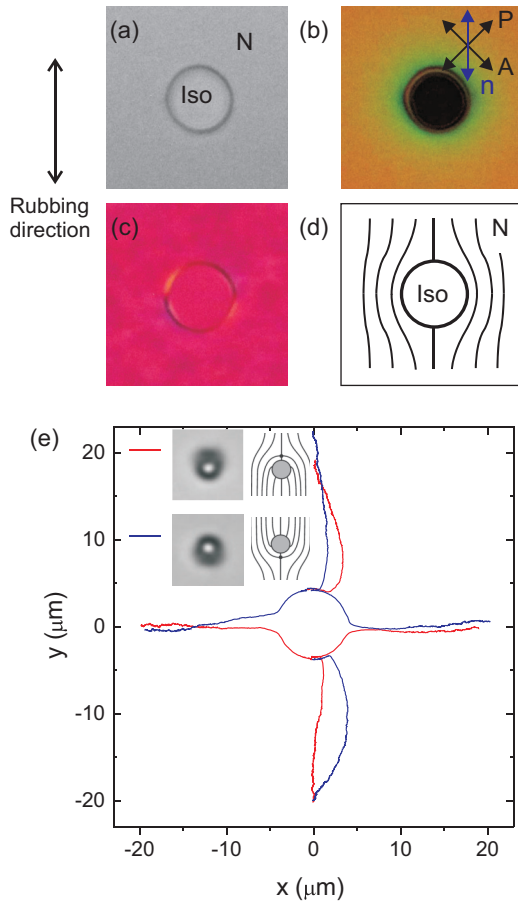


FIG. 3. (Color online) (a) At room temperature, a $\sim 5\text{-}\mu\text{m}$ planar layer of 5CB LC between two ITO-coated glass plates can be locally heated to the isotropic phase with laser tweezers with the power of 30 mW. (b) The birefringence of the LC around the isotropic bubble is changed due to the decreased order parameter and (c) the weak planar orientation at the isotropic-nematic interface can be observed between crossed polarizers with the additional red waveplate. (d) Schematic presentation of LC orientation around the isotropic bubble. (e) The trapping trajectories for two orientations of the $2.32\text{-}\mu\text{m}$ dipolar colloidal particle are not completely isotropic and their shape depends on the orientation of topological dipole.

qualitative agreement between the separation dependence of the trapping potential and the order parameter profile from Fig. 1(c). The trapping effect is stronger if a higher laser power is used. When the laser power is increased to $P \approx 60$ mW, the E12 LC is locally heated to the isotropic phase, the gradient of the order parameter is higher, and the maximum trapping force on the particle is much stronger ($F_{\max} \approx 10$ pN).

We repeated the same experiments with 5CB LC with a lower clearing point $T_c = 34^\circ\text{C}$ compared to E12 with $T_c = 60^\circ\text{C}$. In the case of 5CB the same trapping force is achieved already for much lower laser power (18 mW) because at room temperature the sample is closer to the clearing point and for the same $\Delta S/\Delta y$ less heating is needed. At a laser power of $P = 30$ mW the heating is so intense that a small island of the isotropic phase of 5CB can be seen under an optical microscope [Fig. 3(a)]. In this case the sample is at room temperature closer to T_c and the same amount of absorbed light causes a bigger change of the nematic order

and a bigger change of the LC birefringence [Fig. 3(b)]. In addition to the change of the magnitude of the nematic order, the LC molecules in the interior are also tilted from the rubbing direction due to their planar anchoring at the nematic-isotropic interface, which is schematically presented in Fig. 3(d). This planar orientation at the interface can be observed under crossed polarizers with an additional red waveplate retarder, where blue and yellow colors correspond to two mirror directions of the tilt [Fig. 3(c)].

The colloidal trapping by a small isotropic island in 5CB is much more effective compared to the trapping in E12, where the gradient of S is smaller, but in 5CB the trapping trajectories are not completely isotropic [Fig. 3(e)]. This anisotropy is probably the consequence of the elastic deformation of the nematic director between strongly anchored LC molecules at the surface of the particles and the LC molecules planarly anchored at the nematic-isotropic interface, similar to the case of interactions between different kind of colloids [28]. To prove the elastic origin of this anisotropy, particles with two opposite positions of the point defect and consequently two mirrorlike orientation of the director field were used and trapping trajectories are in both cases in agreement with LC orientation around the particle and around the isotropic bubble. A similar anisotropy of the interactions can be observed between two particles with planar and homeotropic anchoring. We should mention that we did not observe strong anisotropy of trapping trajectories as observed before [21], where the anisotropy of the trapping was explained by the flexoelectric effect.

To understand the mechanism of trapping more clearly we compared the trapping of a silanated silica particle with strong perpendicular surface anchoring and trapping of untreated silica particles with weak planar anchoring. Their trapping potentials, which are calculated as the integral of the trapping force along the trapping trajectory [10], are presented in Fig. 4(a). It is clear that the trapping is more efficient for the particles with stronger surface anchoring, which induce a bigger deformation of the director field [Fig. 4(a), inset]. The elastic energy of the nematic field around the particle is bigger for the particles with stronger surface anchoring and these particles are more strongly attracted into the laser trap.

In addition we have also checked the effect of the particle size on the trapping potential. Figure 4(b) presents the dependence of the maximum trapping potential W_0 on the size of the dipolar particle with strong perpendicular anchoring. The dependence is nearly linear, indicating that the trapping potential is related to the elastic energy of the dipolar particle, which is linearly dependent on the diameter of the particle $W \approx 13\pi K R$ [30]. Here K is an average elastic constant of the nematic and R is the radius of the particle. It is evident from this expression that the elastic energy of the dipolar colloid particle decreases if the particle moves from the region with higher nematic elasticity K (lower temperature and higher order parameter) to the region with lower nematic elasticity K (higher temperature and lower order parameter). We therefore expect that the particle is driven into the hotter region, where the LC is softer and the particle's elastic energy is lower.

By measuring the decrease of the nematic order (Fig. 1) we can estimate the increase of the temperature in the center

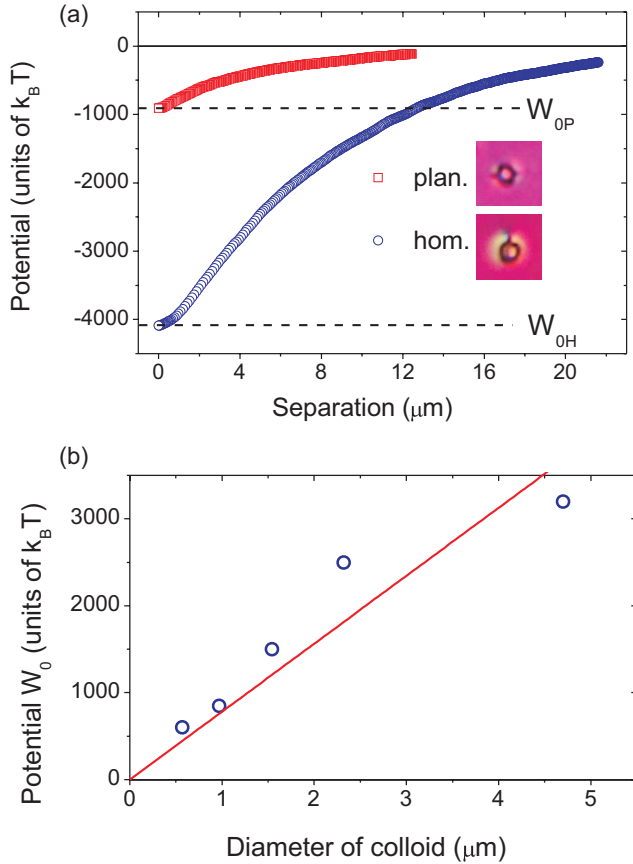


FIG. 4. (Color online) (a) Trapping potentials of untreated silica colloid particles with weak planar anchoring and silanated silica particles with strong homeotropic anchoring in 5CB. The laser power is 22 mW and the particle's diameter is $2.32 \mu m$. The trapping is stronger for the particle with stronger anchoring ($W_{OH} > W_{OP}$), which induces a bigger deformation of the nematic field around the particle. (b) The depth of the trapping potential W_0 for particles with strong homeotropic anchoring is proportional to the diameter of the particle. The solid red line is the best linear fit through the origin. The measured value for the trapping potential of the largest particle is lower than expected from the linear fit. This is probably due to the screening of the potential by the confinement [29]. The laser power is 17 mW.

of the trap with respect to the temperature far away from the trap $\Delta T \approx 2 \text{ K}$ [31]. This means that the average elastic constant of the LC at the position of the trap is decreased by $\Delta K \approx 0.4 \times 10^{-12} \text{ N}$ with respect to the elastic constant far away from the trap [32]. This means that the elastic energy of a dipolar colloid particles with a diameter of $2.32 \mu m$ decreases for $\Delta W \approx 6000 k_B T$, when it is brought from a very large separation into the optical trap, all due to decreased elasticity of the nematic LC in hotter regions. This is actually the depth of the expected trapping potential due to the thermal gradient, which is comparable to the experimentally measured value of the trapping potential $W_0 = 4000 k_B T$. Our experiments therefore clearly show that the trapping mechanism is due to the spatial gradient of the nematic order parameter and reduced elastic energy of dipolar elastic colloids in hotter regions of the nematic LC.

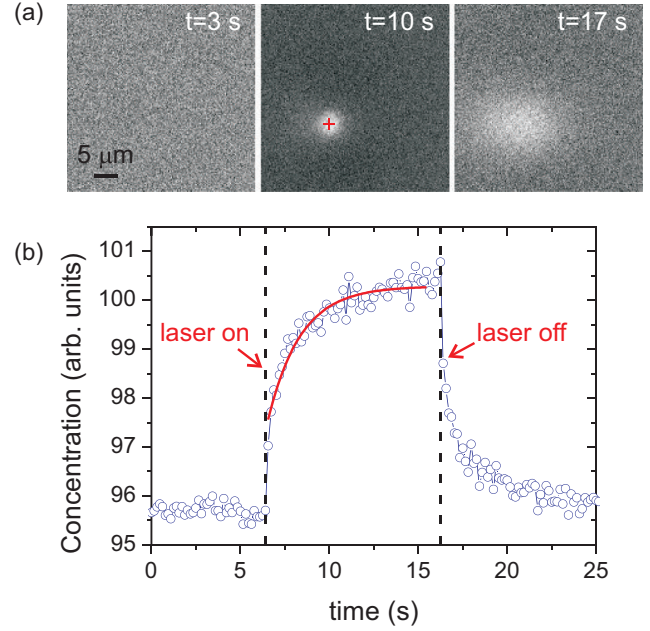


FIG. 5. (Color online) Trapping of dye molecules in 5CB nematic by local heating. (a) Time sequence of fluorescent images before and after switching off the laser tweezers with the power of $P \approx 25 \text{ mW}$, when the LC is heated at the center of the beam close to the isotropic phase. The fluorescent signal is proportional to the dye concentration. (b) The increase of the concentration of dye molecules at the center of the beam is around 5%. The dye concentration changes with the response time $\tau \approx 2 \text{ s}$.

Now there is a question of whether we can see the same trapping mechanism for very small particles, such as fluorescent molecules, with a structure that is different from the structure of LC molecules? To elucidate this, the 5CB LC was doped with rhodamine B fluorescent dye, put in a cell made of ITO-covered glass plates, and irradiated with a focused IR beam of laser tweezers. Fluorescent rhodamine B dye molecules are different from 5CB molecules, which means that their inclusion always creates local disorder of the NLC. Rhodamine B molecules therefore act as nanoparticles, which locally decrease the order parameter, and it is preferable for the free-energy of the system if these disturbing molecules are in the regions of the lower order parameter. Because these are fluorescent molecules, they can easily be observed using fluorescent microscopy.

Figure 5(a) presents a time sequence of fluorescent images taken during an experiment, where the IR laser trap was held at a fixed point and then switched on and off. After switching on the laser trap the dye concentration is increased at the center of the laser trap, where the nematic order parameter is minimal and a bright fluorescent circular region filled with rhodamine molecules is clearly visible [middle panel in Fig. 5(a)]. When the laser is switched off, the fluorescent molecules diffuse away from the concentrated region, diminishing the brightness of the fluorescent circle, which broadens and finally disappears. It should be noted that the fluorescence of rhodamine B diminishes with increasing temperature and the background gets darker when the laser is turned on and the whole sample is heated.

The time dependence of the dye concentration during switching on and off of the laser can be fitted to the exponential function and corresponding response times are below 2 s [Fig. 5(b)]. The fit is not perfect due to the temperature-dependent fluorescence, but we can nevertheless estimate that the concentration of dye molecules at the center of the laser spot is increased for $\approx 5\%$. The experiment was repeated with different dye concentrations and the relative increase of dye concentration at the laser spot was the same, while the absolute value of the fluorescent signal was always proportional to the dye concentration. We also performed the same experiment in the isotropic phase and no increase of the fluorescent signal at the laser spot was observed. We can therefore speculate that the trapping effect in the case of dye molecules is the same as in the case of microparticles. It is, however, also possible that the increased density of dye molecules in the hottest region is caused by the thermal diffusion or Soret effect [33]. In this case the thermodiffusion coefficient in the nematic phase should be significantly different from that in the isotropic phase.

IV. CONCLUSION

We reported the observation of a thermally induced structural force in the nematic liquid crystal, which is due to a spatially inhomogeneous nematic order parameter. These inhomogeneities of the order parameter are very efficient trapping sites for micrometer colloids as well as for nanometer-size fluorescent molecules dispersed in the nematic LC. Thermal manipulation of nematic colloids and even nanocolloids is another phenomenon in a long series of interesting and potentially useful methods of transport of particles in nematic liquid crystals. Further studies should elucidate to what extent the transport can be localized in space and to what complexity it can be structured.

ACKNOWLEDGMENTS

This work was supported by the Slovenian Research Agency (ARRS) under Contracts No. P1-0099 and No. J1-3612 and in part by the Center of Excellence NAMASTE.

-
- [1] J.-i. Hotta, K. Sasaki, and H. Masuhara, *Appl. Phys. Lett.* **71**, 2085 (1997).
 - [2] S. Juodkazis, M. Iwashita, T. Takahashi, S. Matsuo, and H. Misawa, *Appl. Phys. Lett.* **74**, 3627 (1999).
 - [3] S. Juodkazis, S. Matsuo, N. Murazawa, I. Hasegawa, and H. Misawa, *Appl. Phys. Lett.* **82**, 4657 (2003).
 - [4] T. A. Wood, H. F. Gleeson, M. R. Dickinson, and A. J. Wright, *Appl. Phys. Lett.* **84**, 4292 (2004).
 - [5] H. F. Gleeson, T. A. Wood, and M. Dickinson, *Philos. Trans. R. Soc. London Ser. A* **364**, 2789 (2006).
 - [6] Y. Iwashita and H. Tanaka, *Phys. Rev. Lett.* **90**, 045501 (2003).
 - [7] M. Yada, J. Yamamoto, and H. Yokoyama, *Phys. Rev. Lett.* **92**, 185501 (2004).
 - [8] I. I. Smalyukh, A. N. Kuzmin, A. V. Kachynski, P. N. Prasad, and O. D. Lavrentovich, *Appl. Phys. Lett.* **86**, 021913 (2005).
 - [9] I. Muševič, M. Škarabot, D. Babič, N. Osterman, I. Poberaj, V. Nazarenko, and A. Nych, *Phys. Rev. Lett.* **93**, 187801 (2004).
 - [10] M. Škarabot, M. Ravnik, D. Babič, N. Osterman, I. Poberaj, S. Žumer, I. Muševič, A. Nych, U. Ognysta, and V. Nazarenko, *Phys. Rev. E* **73**, 021705 (2006).
 - [11] B. Lev, A. Nych, U. Ognysta, S. B. Chernyshuk, V. Nazarenko, M. Škarabot, I. Poberaj, D. Babič, N. Osterman, and I. Muševič, *Eur. Phys. J. E* **20**, 215 (2006).
 - [12] J. Kotar, M. Vilfan, N. Osterman, D. Babič, M. Čopič, and I. Poberaj, *Phys. Rev. Lett.* **96**, 207801 (2006).
 - [13] I. Smalyukh, A. V. Kachynski, A. N. Kuzmin, and P. N. Prasad, *Proc. Natl. Acad. Sci. USA* **103**, 18048 (2006).
 - [14] L. Lucchetti, L. Criante, F. Bracalente, F. Aieta, and F. Simoni, *Phys. Rev. E* **84**, 021702 (2011).
 - [15] O. P. Pishnyak, S. Tang, J. R. Kelly, S. V. Shiyankovskii, and O. D. Lavrentovich, *Phys. Rev. Lett.* **99**, 127802 (2007).
 - [16] M. Škarabot, U. Tkalec, and I. Muševič, *Eur. Phys. J. E* **24**, 99 (2007).
 - [17] A. V. Ryzhkova, F. V. Podgornov, and W. Haase, *Appl. Phys. Lett.* **96**, 151901 (2010).
 - [18] O. D. Lavrentovich, I. Lazo, and O. P. Pishnyak, *Nature (London)* **467**, 947 (2010).
 - [19] J. L. West, A. Glushchenko, G. X. Liao, Y. Reznikov, D. Andrienko, and M. P. Allen, *Phys. Rev. E* **66**, 012702 (2002).
 - [20] A. Sengupta, U. Tkalec, and C. Bahr, *Soft Matter* **7**, 6542 (2011).
 - [21] S. A. Tatarkova, D. R. Burnham, A. K. Kirby, G. D. Love, and E. M. Terentjev, *Phys. Rev. Lett.* **98**, 157801 (2007).
 - [22] Y. Galerne, *Phys. Rev. Lett.* **101**, 029801 (2008).
 - [23] S. A. Tatarkova, D. R. Burnham, A. K. Kirby, G. D. Love, and E. M. Terentjev, *Phys. Rev. Lett.* **101**, 029802 (2008).
 - [24] S. Samitsu, Y. Takanishi, and J. Yamamoto, *Nat. Mater.* **9**, 816 (2010).
 - [25] S. T. Wu, *Phys. Rev. A* **33**, 1270 (1986).
 - [26] P. Poulin, V. Cabuil, and D. A. Weitz, *Phys. Rev. Lett.* **79**, 4862 (1997).
 - [27] J. C. Loudet, P. Hanusse, and P. Poulin, *Science* **306**, 1525 (2004).
 - [28] U. Ognysta, A. Nych, V. Nazarenko, I. Muševič, M. Škarabot, M. Ravnik, S. Žumer, I. Poberaj, and D. Babič, *Phys. Rev. Lett.* **100**, 217803 (2008).
 - [29] M. Vilfan, N. Osterman, M. Čopič, M. Ravnik, S. Žumer, J. Kotar, D. Babič, and I. Poberaj, *Phys. Rev. Lett.* **101**, 237801 (2008).
 - [30] H. Stark, *Phys. Rep.* **351**, 387 (2001).
 - [31] S. Sen, P. Brahma, S. K. Roy, D. K. Mukherjee, and S. B. Roy, *Mol. Cryst. Liq. Cryst.* **100**, 327 (1983).
 - [32] M. Hara, J. Hirakata, T. Toyooka, H. Takezoe, and A. Fukuda, *Mol. Cryst. Liq. Cryst.* **122**, 161 (1985).
 - [33] S. Dühr and D. Braun, *Proc. Natl. Acad. Soc.* **103**, 19678 (2006).